

Recurrent Equilibrium Networks: Unconstrained Learning of Stable and Robust Dynamical Models

Max Revay, Ruigang Wang, Ian R. Manchester

Abstract—This paper introduces *recurrent equilibrium networks* (RENs), a new class of nonlinear dynamical models for applications in machine learning and system identification. The new model class has “built in” guarantees of stability and robustness: all models in the class are contracting – a strong form of nonlinear stability – and models can have prescribed Lipschitz bounds. RENs are otherwise very flexible: they can represent all stable linear systems, all previously-known sets of contracting recurrent neural networks, all deep feedforward neural networks, and all stable Wiener/Hammerstein models. RENs are parameterized directly by a vector in \mathbb{R}^N , i.e. stability and robustness are ensured without parameter constraints, which simplifies learning since generic methods for unconstrained optimization can be used. The performance of the robustness of the new model set is evaluated on benchmark nonlinear system identification problems.

I. INTRODUCTION

Learning nonlinear dynamical systems from data is a common problem in the sciences and engineering, and a wide range of model classes have been developed, including finite impulse response models [1] and models that contain feedback, e.g. nonlinear state-space models [2], autoregressive models [3] and recurrent neural networks [4].

When learning models with feedback it is not uncommon for the model to be unstable even if the data-generating system is stable, and this has led to a large volume of research on guaranteeing model stability. Even in the case of linear models the problem is complicated by the fact that the set of stable matrices is non-convex, and various methods have been proposed to guarantee stability via regularisation and constrained optimisation [5], [6], [7], [8], [9], [10], [11].

For nonlinear models, there has also been a substantial volume of research on stability guarantees, e.g. for polynomial models [12], [13], [14], [15], Gaussian mixture models [16], and recurrent neural networks [17], [10], [18], [19], [20], however the problem is substantially more complex than the linear case as there are many different definitions of nonlinear stability and even verification of stability of a given model is challenging. Contraction is a strong form of nonlinear stability [21], which is particularly well-suited to problems in learning and system identification since it guarantees stability of *all* solutions of the model, irrespective of inputs or initial conditions. This is important in learning since the purpose of a model is to simulate responses to previously unseen inputs. In particular, the works [12], [13],

[14], [15], [17], [19], [20] are guaranteed to find contracting models.

Beyond stability, model *robustness* can be characterised in terms of sensitivity to small perturbations in the input. It has recently been shown that recurrent neural network models can be extremely fragile [22], i.e. small changes to the input produce dramatic changes in the output, raising concerns when using these components in a safety critical context where stability and robustness are key concerns.

Formally, sensitivity and robustness can be quantified via *Lipschitz bounds* on the input-output mapping defined by the model, e.g. incremental ℓ_2 gain bounds which have a long history in systems analysis [23]. In machine learning, Lipschitz constants are used in the proofs of generalization bounds [24], analysis of expressiveness [25] and guarantees of robustness to adversarial attacks [26], [27]. There is also ample empirical evidence to suggest that Lipschitz regularity (and model stability, where applicable) improves generalization in machine learning [28], system identification [29] and reinforcement learning [30].

Unfortunately, even calculation of the Lipschitz constant of a feedforward (static) neural networks is NP-hard [31] and instead approximate bounds must be used. The tightest bound known to date is found by using quadratic constraints to construct a behavioural description of the neural network activation functions [32]. Extending this approach to network synthesis (i.e., training new neural networks with a prescribed Lipschitz bound) is complicated by as the model parameters and IQC multipliers are not jointly convex. In [33], Lipschitz bounded feedforward models were trained using the Alternating Direction Method of Multipliers, and in [29], a convexifying implicit parametrization and an interior point method were used to train Lipschitz bounded recurrent neural networks. Empirically, both works suggest generalisation and robustness advantages to Lipschitz regularisation, however, the requirements to satisfy linear matrix inequalities at each iteration mean that these methods are limited to relatively small scale networks.

In this work, we build dynamical models incorporating a new class of neural network models: equilibrium networks [34] a.k.a. implicit deep networks [35]. These models operate on the fixed points of implicit neural network equations, and can be shown to contain many prior network structures as special cases [35]. Well-posedness (solvability) conditions for these implicit equations have recently developed based on monotone operator theory [36] and contraction analysis [37], while the latter also allowed prescribed bounds on Lipschitz constants. A benefit of the formulations in [36]

This work was supported by the Australian Research Council.

The authors are with the Australian Centre for Field Robotics and Sydney Institute for Robotics and Intelligent Systems, The University of Sydney, Sydney, NSW 2006, Australia (e-mail: ian.manchester@sydney.edu.au).

and [37] is that they permit a *direct* parametrization, i.e. there are mappings directly from \mathbb{R}^N for some N to models that automatically satisfies the well-posedness and robustness constraints, allowing learning via unconstrained optimization methods that scale to large-scale problems such as stochastic gradient descent.

A. Contributions

In this work we propose *recurrent equilibrium networks* (RENs), a new model class of robust nonlinear dynamical systems constructed via a feedback interconnection between a linear dynamical system and an equilibrium neural network. This model class has the following benefits:

- RENs have “built in” stability (contraction) and robustness (Lipschitz boundedness) guarantees.
- RENs are flexible: the model class contains all stable linear models, all previously-known sets of contracting recurrent neural networks, feedforward neural networks of arbitrary depth, nonlinear finite-impulse response models, and block-structured models such as Wiener and Hammerstein models.
- RENs admit a *direct parameterization*, i.e. a mapping from \mathbb{R}^N to models with stability and robustness guarantees, thus enabling learning via unconstrained optimisation.

Finally, we explore performance and robustness of the proposed model set on two benchmark nonlinear system identification problems, comparing to standard RNNs and Long Short Term Memory (LSTM) [38], a widely-used class of recurrent models designed to be stable and easy to train.

B. Notation

The set of sequences $x : \mathbb{N} \rightarrow \mathbb{R}^n$ is denoted by ℓ_{2e}^n . Superscript n is omitted when it is clear from the context. For $x \in \ell_{2e}^n$, $x_t \in \mathbb{R}^n$ is the value of the sequence x at time $t \in \mathbb{N}$. The subset $\ell_2 \subset \ell_{2e}$ consists of all square-summable sequences, i.e., $x \in \ell_2$ if and only if the ℓ_2 norm $\|x\| := \sqrt{\sum_{t=0}^{\infty} |x_t|^2}$ is finite, where $|\cdot|$ denotes Euclidean norm. Given a sequence $x \in \ell_{2e}$, the ℓ_2 norm of its truncation over $[0, T]$ is $\|x\|_T := \sqrt{\sum_{t=0}^T |x_t|^2}$. For matrices A , we use $A \succ 0$ and $A \succeq 0$ to mean A is positive definite or positive semi-definite respectively. We denote the set of positive-definite matrices and diagonal positive-definite matrices by \mathbb{S}_+ and \mathbb{D}_+ , respectively.

II. LEARNING STABLE AND ROBUST MODELS

Given the training data set $\tilde{z} = \{\tilde{u}, \tilde{y}\}$ where $\tilde{u} \in \ell_{2e}^m$ and $\tilde{y} \in \ell_{2e}^p$ denote the sequences of input and output with some finite length T , respectively, we aim to learn a nonlinear state-space dynamical model of the form

$$x_{t+1} = f(x_t, u_t, \theta), \quad y_t = g(x_t, u_t, \theta) \quad (1)$$

where $x_t \in \mathbb{R}^n$, $u_t \in \mathbb{R}^m$, $y_t \in \mathbb{R}^p$, $\theta \in \mathbb{R}^N$ are the state, input, output and model parameter, respectively. Here $f : \mathbb{R}^n \times \mathbb{R}^m \times \mathbb{R}^N \rightarrow \mathbb{R}^n$ and $g : \mathbb{R}^n \times \mathbb{R}^m \times \mathbb{R}^N \rightarrow \mathbb{R}^p$ are piecewise continuously differentiable functions.

Model training can be formulated as an optimization problem as follows:

$$\min_{\theta \in \Theta \subset \mathbb{R}^N} L(\tilde{z}, x, \theta) \quad (2)$$

where $L(\tilde{z}, x, \theta)$ denotes the fitting error (i.e. loss function). There are many choices, but the most straightforward one is the *simulation error*, i.e. $L(\tilde{z}, x, \theta) = \|y - \tilde{y}\|_T^2$ where $y = S_a(\tilde{u})$ is the output sequence generated by the nonlinear dynamical model (1) with initial condition $x_0 = a$ and inputs $u_t = \tilde{u}_t$.

Definition 1: A model parameterization (1) is called a *direct parameterization* if $\Theta = \mathbb{R}^N$.

Direct parameterizations are useful for learning large-scale models since many scalable unconstrained optimization methods (e.g. stochastic gradient descent) can be applied to solve the learning problem (2).

In this paper, we are interested in constructing direct parameterized model sets with certain robustness properties. To formally define robustness, we first recall some strong stability notions from [20].

Definition 2: A model (1) is said to be *contracting* if for any two initial conditions $a, b \in \mathbb{R}^n$, given the same input sequence $u \in \ell_{2e}^m$, the state sequences x^a and x^b satisfy $\|x_t^a - x_t^b\| \leq R\alpha^t \|a - b\|$ for some $R > 0$ and $\alpha \in [0, 1)$.

Definition 3: A model (1) is said to have an *incremental* ℓ_2 -gain bound of γ if for all pairs of solutions with initial conditions $a, b \in \mathbb{R}^n$ and input sequences $u^a, u^b \in \ell_{2e}^m$, the output sequences $y^a = S_a(u^a)$ and $y^b = S_b(u^b)$ satisfy

$$\|y^a - y^b\|_T^2 \leq \gamma^2 \|u^a - u^b\|_T^2 + d(a, b), \quad \forall T \in \mathbb{N}, \quad (3)$$

for some function $d(a, b) \geq 0$ with $d(a, a) = 0$.

Definition 2 implies that initial conditions are forgotten exponentially. Definition 3 not only guarantees the effect of initial condition on the output are forgotten but also implies that all sequence-to-sequence operator S_a have a Lipschitz bound of γ , i.e.,

$$\|S_a(u) - S_a(v)\|_T \leq \gamma \|u - v\|_T, \quad \forall u, v \in \ell_{2e}^m, T \in \mathbb{N}. \quad (4)$$

As illustrated in [39], [19], [20], the learned model with above stability constraints can have predictable response to a wide variety of unseen inputs independent of model initial conditions.

III. RECURRENT EQUILIBRIUM NETWORKS

We construct the model (1) as a feedback interconnection of a linear system G and a static, memoryless nonlinear operator σ , as depicted in Fig. 1:

$$\begin{bmatrix} E x_{t+1} \\ \Lambda v_t \\ y_t \end{bmatrix} = \overbrace{\begin{bmatrix} F & B_1 & B_2 \\ C_1 & D_{11} & D_{12} \\ C_2 & D_{21} & D_{22} \end{bmatrix}}^W \begin{bmatrix} x_t \\ w_t \\ u_t \end{bmatrix} + \overbrace{\begin{bmatrix} b_x \\ b_v \\ b_y \end{bmatrix}}^b, \quad (5)$$

$$w_t = \sigma(v_t) := [\sigma(v_t^1) \quad \sigma(v_t^2) \quad \dots \quad \sigma(v_t^q)]^\top, \quad (6)$$

where $v_t, w_t \in \mathbb{R}^q$ are the input and output of neurons respectively, $E \in \mathbb{R}^{n \times n}$, $\Lambda \in \mathbb{D}_+^q$, $W \in \mathbb{R}^{(n+p+q) \times (n+m+q)}$

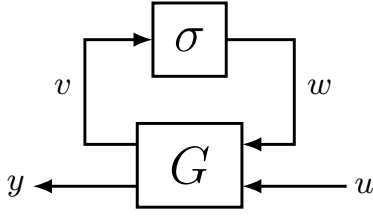


Fig. 1. REN as a feedback interconnection of a linear system G and a nonlinear activation σ .

are weight matrices, and $b \in \mathbb{R}^{n+p+q}$ is the bias vector. We assume that $\sigma: \mathbb{R} \rightarrow \mathbb{R}$ is a single nonlinear activation function applied elementwise. The results can be directly applied to the case where each channel has a different activation function, linear or nonlinear. We also make the following assumption on σ , which holds for most activation functions in literature [40].

Assumption 1: The activation function σ is piecewise differentiable and slope-restricted in $[0, 1]$, i.e.,

$$0 \leq \frac{\sigma(y) - \sigma(x)}{y - x} \leq 1, \quad \forall x, y \in \mathbb{R}, x \neq y. \quad (7)$$

We refer to the model (5), (6) as a *recurrent equilibrium network* (REN) as the feedback interconnection contains an implicit or equilibrium network ([34], [36], [37], [35]):

$$w_t = \sigma(Dw_t + b_w) \quad (8)$$

with $D = \Lambda^{-1}D_{11}$ and $b_w = \Lambda^{-1}(C_1x_t + D_{12}u_t + b_w)$. The term ‘‘equilibrium’’ is from the fact that any solution w_t^* of the above equation is also an equilibrium point of the difference equation $w_t^{k+1} = \sigma(Dw_t^k + b_w)$ or the neural ODE $\frac{d}{ds}w_t(s) = -w_t(s) + \sigma(Dw_t(s) + b_w)$.

One of the central results in [37] is that (8) is well-posed (i.e., a unique solution w_t^* exists for all input b_w) if there exists a $\Psi \in \mathbb{D}_+^n$ such that

$$2\Psi - \Psi D - D^\top \Psi \succ 0. \quad (9)$$

A well-posed equilibrium network can be linked to an operator splitting problem via monotone operator theory [41] or a contracting dynamical system via IQC analysis framework [42]. Thus, various of numerical methods can be applied for solving an equilibrium, e.g., operator splitting algorithm or ODE solvers, see [37].

When training an equilibrium network via gradient decent, we need to compute the Jacobian $\partial w_t^*/\partial(\cdot)$ where w_t^* is the solution of the implicit equation (8), (\cdot) denotes the input to the network or parameters. By using implicit function theorem, $\partial w_t^*/\partial(\cdot)$ can be computed via

$$\frac{\partial w_t^*}{\partial(\cdot)} = (I - JD)^{-1}J \frac{\partial(Dw_t^* + b_w)}{\partial(\cdot)} \quad (10)$$

where J is the Clarke generalized Jacobian of σ at $Dw_t^* + b_w$. From Assumption 1, we have that J is a singleton almost everywhere. In particular, J is a diagonal matrix satisfying $0 \preceq J \preceq I$. The matrix $I - JD$ is invertible by Condition (9) [37].

IV. DIRECT PARAMETERIZATIONS OF RENS

In this section, we first give two direct parameterized robust REN model set, namely contracting REN (C-REN) and Lipschitz bounded REN (LB-REN). Then, we show that the proposed model sets are very flexible as they contain many prior model structures as special cases.

A. Contracting RENS

Letting \mathcal{M}_* be the set of C-RENS, we give one of its direct parameterizations as follows. First, consider the parameter vector θ consisted of $A \in \mathbb{R}^{2n+q}$, $l \in \mathbb{R}^q$, $B_1 \in \mathbb{R}^{n \times q}$, $B_2 \in \mathbb{R}^{n \times m}$, $C_2 \in \mathbb{R}^{p \times n}$, $D_{12} \in \mathbb{R}^{q \times m}$, $D_{21} \in \mathbb{R}^{p \times q}$, $D_{22} \in \mathbb{R}^{p \times m}$, $S_1 \in \mathbb{R}^{n \times n}$ and $S_2 \in \mathbb{R}^{q \times q}$. The weight matrices of models in \mathcal{M}_* are then given by

$$E = \frac{1}{2}(H_{11} + P + S_1 - S_1^\top), \quad F = H_{31}, \quad \Lambda = e^{\text{diag}(l)}$$

$$C_1 = -H_{21}, \quad D_{11} = \Lambda - \frac{1}{2}(H_{22} + S_2 - S_2^\top), \quad B_1 = H_{32}$$

where $P = H_{33}$ and

$$H = \begin{bmatrix} H_{11} & H_{12} & H_{13} \\ H_{21} & H_{22} & H_{23} \\ H_{31} & H_{32} & H_{33} \end{bmatrix} = A^\top A + \epsilon I \quad (11)$$

with $H_{11}, H_{33} \in \mathbb{S}_+^n$ and $H_{22} \in \mathbb{S}_+^q$. Here ϵ is chosen to be a small positive constant such that H is strictly positive.

Now we are ready to state our first main result.

Theorem 1: All models in \mathcal{M}_* are contracting.

Proof: For any two sequences $z^a = (x^a, w^a, v^a)$ and $z^b = (x^b, w^b, v^b)$ generated by (1) with initial states a, b and the same input u , the error dynamics of $\Delta z_t := z_t^a - z_t^b$ can be represented by

$$\begin{bmatrix} E\Delta x_{t+1} \\ \Lambda\Delta v_t \end{bmatrix} = \begin{bmatrix} F & B_1 \\ C_1 & D_{11} \end{bmatrix} \begin{bmatrix} \Delta x_t \\ \Delta w_t \end{bmatrix}, \quad (12)$$

$$\Delta w_t = \sigma(v_t + \Delta v_t) - \sigma(v_t). \quad (13)$$

By taking a conic combination of incremental sector-bounded constraints (7) on each channel, the relationship in (13) satisfies the following quadratic constraint

$$Q_t = \begin{bmatrix} \Delta v_t \\ \Delta w_t \end{bmatrix}^\top \begin{bmatrix} 0 & \Lambda \\ \Lambda & -2\Lambda \end{bmatrix} \begin{bmatrix} \Delta v_t \\ \Delta w_t \end{bmatrix} \geq 0 \quad \forall t \in \mathbb{N}. \quad (14)$$

From the model parameterization, it is easy to verify that \mathcal{M}_* satisfies

$$\begin{bmatrix} E + E^\top - P & -C_1^\top & F^\top \\ -C_1 & \mathcal{W} & B_1^\top \\ F & B_1 & P \end{bmatrix} \succ 0, \quad (15)$$

where $\mathcal{W} = 2\Lambda - D_{11} - D_{11}^\top$. By Schur complement we have

$$\begin{bmatrix} E + E^\top - P & -C_1^\top \\ -C_1 & \mathcal{W} \end{bmatrix} - \begin{bmatrix} F^\top \\ B_1^\top \end{bmatrix} P^{-1} \begin{bmatrix} F^\top \\ B_1^\top \end{bmatrix} \succ 0.$$

By applying the inequality $E^\top P^{-1} E \succeq E + E^\top - P$ and left-multiplying $[\Delta x_t^\top \quad \Delta w_t^\top]$ and right-multiplying

$[\Delta x_t^\top \ \Delta w_t^\top]^\top$, we obtain the following incremental Lyapunov inequality:

$$V_{t+1} - V_t \leq -Q_t \leq 0, \quad (16)$$

where $V_t = \Delta x_t^\top E^\top P^{-1} E \Delta x_t$. Since V_t is a quadratic form in Δx_t , it follows that $V_{t+1} \leq \alpha V_t$ for some $\alpha \in [0, 1)$ and $V_t \leq \alpha^t V_0$. ■

Remark 1: The incremental quadratic constraint (14) generally does not hold for the richer (more powerful) class of multipliers for repeated nonlinearities [43], [44], [45] since Δw_t^i explicitly depend on the value of v_t^i which may differ among channels [37].

Proposition 1: All models in \mathcal{M}_* are well-posed, i.e., (5), (6) yield a unique solution (w_t, x_{t+1}) for any x_t, u_t and b .

Proof: From (15) we have $E + E^\top \succ P \succ 0$ and $\mathcal{W} = 2\Lambda - \Lambda\Lambda^{-1}D_{11} - D_{11}^\top\Lambda^{-1}\Lambda \succ 0$. The first LMI implies that E is invertible [39] and thus (5) is well-posed. The second one ensures that the equilibrium network (8) is well-posed. ■

B. Lipschitz bounded RENs

In this section, we give a direct parameterization for the model set \mathcal{M}_γ , where \mathcal{M}_γ denotes the set of LB-RENs with Lipschitz bound γ . First, we choose the model parameter θ as the union of following free variables: $A \in \mathbb{R}^{2n+q}$, $l \in \mathbb{R}^q$, $B_2 \in \mathbb{R}^{n \times m}$, $C_2 \in \mathbb{R}^{p \times n}$, $D_{12} \in \mathbb{R}^{q \times m}$, $D_{21} \in \mathbb{R}^{p \times q}$, $S_1 \in \mathbb{R}^{n \times n}$ and $S_2 \in \mathbb{R}^{q \times q}$. The weight matrices of models in \mathcal{M}_γ are given by

$$E = \frac{1}{2} \left(H_{11} + \frac{1}{\gamma} C_2^\top C_2 + P + S_1 - S_1^\top \right),$$

$$F = H_{31}, \quad D_{22} = 0, \quad \Lambda = e^{\text{diag}(l)},$$

$$B_1 = H_{32} - \frac{1}{\gamma} B_2 D_{12}^\top, \quad C_1 = - \left(H_{21} + \frac{1}{\gamma} D_{21}^\top C_2 \right),$$

$$D_{11} = \Lambda - \frac{1}{2} \left(H_{22} + \frac{1}{\gamma} D_{21}^\top D_{21} + \frac{1}{\gamma} D_{21} D_{12}^\top + S_2 - S_2^\top \right),$$

where $P = H_{33} + \frac{1}{\gamma} B_2^\top B_2$ with H defined in (11).

Theorem 2: All models in \mathcal{M}_γ have an Lipschitz bound of γ .

Proof: For any two trajectories $z = (x, w, v, u, y)$ and $z' = (x', w', v', u', y')$, the error dynamics of $\Delta z_t := z'_t - z_t$ can be represented by

$$\begin{bmatrix} E\Delta x_{t+1} \\ \Lambda\Delta v_t \\ \Delta y_t \end{bmatrix} = \begin{bmatrix} F & B_1 & B_2 \\ C_1 & D_{11} & D_{12} \\ C_2 & D_{21} & D_{22} \end{bmatrix} \begin{bmatrix} \Delta x_t \\ \Delta w_t \\ \Delta u_t \end{bmatrix}. \quad (17)$$

Here the sequences Δw and Δv also satisfy the relationship (13), which further implies that the quadratic constraint (14) holds.

Simple computation shows that \mathcal{M}_γ satisfies

$$\begin{bmatrix} E + E^\top - P & -C_1^\top & F^\top \\ -C_1 & \mathcal{W} & B_1^\top \\ F & B_1 & P \end{bmatrix} - \frac{1}{\gamma} \begin{bmatrix} 0 & C_2^\top \\ -D_{12} & D_{21}^\top \\ B_2 & 0 \end{bmatrix}^\top \begin{bmatrix} 0 & C_2^\top \\ -D_{12} & D_{21}^\top \\ B_2 & 0 \end{bmatrix} \succ 0$$

By applying Schur complement to the above inequality, we obtain that

$$\begin{bmatrix} E + E^\top - P & -C_1^\top & F^\top & 0 & C_2^\top \\ -C_1 & \mathcal{W} & B_1^\top & -D_{12} & D_{21}^\top \\ F & B_1 & P & B_2 & 0 \\ 0 & -D_{12}^\top & B_2^\top & \gamma I & D_{22}^\top \\ C_2 & D_{21} & 0 & D_{22} & \gamma I \end{bmatrix} \succ 0, \quad (18)$$

which is equivalent to

$$\begin{bmatrix} E + E^\top - P & -C_1^\top & 0 & F^\top & C_2^\top \\ -C_1 & \mathcal{W} & -D_{12} & B_1^\top & D_{21}^\top \\ 0 & -D_{12}^\top & \gamma I & B_2^\top & D_{22}^\top \\ F & B_1 & B_2 & P & 0 \\ C_2 & D_{21} & D_{22} & 0 & \gamma I \end{bmatrix} \succ 0.$$

Two applications of Schur complement with respect to the lower-right block gives

$$\begin{bmatrix} E + E^\top - P & -C_1^\top & 0 \\ -C_1 & \mathcal{W} & -D_{12} \\ 0 & -D_{12}^\top & \gamma I \end{bmatrix} - \begin{bmatrix} F^\top \\ B_1^\top \\ B_2^\top \end{bmatrix} P^{-1} \begin{bmatrix} F^\top \\ B_1^\top \\ B_2^\top \end{bmatrix}^\top - \frac{1}{\gamma} \begin{bmatrix} C_2^\top \\ D_{21}^\top \\ D_{22}^\top \end{bmatrix} \begin{bmatrix} C_2^\top \\ D_{21}^\top \\ D_{22}^\top \end{bmatrix}^\top \succ 0.$$

By applying the inequality $E^\top P^{-1} E \succeq E + E^\top - P$ and left-multiplying $[\Delta x_t^\top \ \Delta w_t^\top \ \Delta u_t^\top]$ and right-multiplying $[\Delta x_t^\top \ \Delta w_t^\top \ \Delta u_t^\top]^\top$, we obtain the following incremental dissipation inequality

$$V_{t+1} - V_t + Q_t \leq \frac{1}{\gamma} |\Delta u_t|^2 - \gamma |\Delta y_t|^2$$

where $V_t = \Delta x_t^\top E P^{-1} E \Delta x_t$. Then, the Lipschitz bound of γ follows by (14). ■

Remark 2: Although the proposed LB-REN model parameterization does not explicitly contain any feed-through term from u to y as $D_{22} = 0$, it could involve the feed-through term implicitly when the learned model takes the input u_t as part of the state x_t , i.e., a non-zero D_{22} is learned as part of the matrix C_2 .

The following proposition shows that all LB-RENs are also contracting.

Proposition 2: All models in $\mathcal{M}_* \supset \mathcal{M}_\gamma$ have a finite Lipschitz bound.

Proof: Since (15) appears as the upper-left block in (18), we have $\mathcal{M}_* \supset \mathcal{M}_\gamma$. As a partial converse, (15) implies that for arbitrary B_2, C_2, D_{12}, D_{21} and D_{22} , there exists a sufficiently large but finite γ such that LMI (18) holds. ■

C. Model Expressivity

The set of RENs contains many prior model structures as a special case. We now discuss the relationship to some prior model types:

1) *Robust and Contracting Recurrent Neural Networks:*

The robust RNN proposed in [20] is a parametrization of RNNs with incremental stability and robustness guarantees. The robust RNN was also shown to contain:

- 1) all stable LTI systems
- 2) all prior sets of contracting RNNs including the ciRNN [19] and s-RNN[17].

The model set \mathcal{M}_* reduces to the model set proposed in [20] whenever $D_{11} = 0$.

2) *Feedforward Neural Networks:* The REN contains many feedforward neural network architectures as a special case. For example, a standard L -layer DNN takes the form

$$z_0 = u, \quad z_{l+1} = \sigma(W_l z_l + b_l), \quad l = 0, \dots, L-1 \quad (19)$$

$$y = W_L z_L + b_L.$$

This can be written as an implicit neural network (5), (6) with

$$w = \text{col}(z_1, \dots, z_L), \quad b_w = \text{col}(b_0, \dots, b_{L-1}), \quad by = b_L$$

$$D_{12} = \text{col}(W_0, 0, \dots, 0), \quad D_{21} = \begin{bmatrix} 0 & \cdots & 0 & W_L \end{bmatrix},$$

$$\Lambda^{-1} D_{11} = \begin{bmatrix} 0 & & & \\ W_1 & \ddots & & \\ \vdots & \ddots & 0 & \\ 0 & \cdots & W_{L-1} & 0 \end{bmatrix}.$$

In [37], it was shown that the set of Lipschitz bounded equilibrium networks contains all models of the form (19) as well as a much larger class of neural networks. The model set \mathcal{M}_* reduces to the model set proposed in [37] when $n = 0$. More generally, \mathcal{M}_* contains any Lipschitz bounded equilibrium of the system state or input.

3) *Block Structured Models:* Block structured models are constructed from LTI systems connected via static nonlinearities [46], [47]. The REN contains block structured models as a subset, where the equilibrium network represents can approximate any continuous static nonlinearity and the linear system represents the LTI block. For simplicity, we only consider two simple block oriented models:

- 1) *Wiener systems* consist of an LTI block followed by a static non-linearity. This structure is replicated in (5), (6) when $B_1 = 0$ and $C_2 = 0$. In this case the linear dynamical system evolves independently of the nonlinearities and feeds into a equilibrium network.
- 2) *Hammerstein systems* consist of a static non-linearity connected to an LTI system. This is represented in the REN when $B_2 = 0$ and $C_1 = 0$. In this case the input passes through a static equilibrium network and into an LTI system.

Other more complex oriented models such as [48] can also be constructed.

4) *Nonlinear Finite Impulse Response Models:* Finite impulse response models are finite memory nonlinear filters. These have a similar construction to Wiener systems, where the LTI system contains a delay system that stores a finite

history of inputs. The REN recovers a set of finite memory filters when

$$E^{-1}F = \begin{bmatrix} 0 & & & \\ 1 & 0 & & \\ & & \ddots & \\ & & & 1 & \ddots & \\ & & & & & \ddots \end{bmatrix}, \quad E^{-1}B_2 = \begin{bmatrix} 1 \\ 0 \\ 0 \\ \vdots \end{bmatrix}, \quad B_1 = 0. \quad (20)$$

The output is then a nonlinear function of a truncated history of inputs.

V. BENCHMARK CASE STUDIES

We demonstrate the proposed model set on the F16 ground vibration [49] and Wiener Hammerstein with process noise [50] system identification benchmark. We will compare the REN_* and REN_γ with an LSTM and RNN with a similar number of parameters.

An advantage of using a direct parametrization is that unconstrained optimization techniques can be applied. We fit models by minimizing simulation error:

$$J_{se}(\theta) = \|\tilde{y} - S_a(\tilde{u})\|_T \quad (21)$$

using minibatch gradient descent with the ADAM optimizer [51].

When simulating the model, we use the Peaceman-Rachford monotone operator splitting algorithm [41], [36], [37] to solve for the fixed points in (8). We use the conjugate gradient method to solve for the gradients with the respect to the equilibrium layer (8). The remaining gradients are calculated using the automatic differentiation tool, Zygote [52].

Model performance is measured using normalised root mean square error on the test sets, calculated as:

$$\text{NRMSE} = \frac{\|\tilde{y} - S_a(\tilde{u})\|_T}{\|\tilde{y}\|_T}. \quad (22)$$

Model robustness is measured in terms of the maximum observed sensitivity:

$$\underline{\gamma} = \max_{u_1, u_2, a} \frac{\|S_a(u_1) - S_a(u_2)\|_T}{\|u_1 - u_2\|_T}. \quad (23)$$

We find a local solution to (23) using gradient ascent with the ADAM optimizer. Consequently $\underline{\gamma}$ is a lower bound on the true Lipschitz constant of the sequence-to-sequence map.

A. Benchmark Datasets and Training Details

1) *F16 System Identification Benchmark:* The F16 ground vibration benchmark data-set [49] consists of accelerations measured by three accelerometers, induced in the structure of an F16 fighter jet by a wing mounted shaker. We use the multisine excitation dataset with full frequency grid. This dataset consists of 7 multisine experiments with 73,728 samples and varying amplitude. We use data-sets 1, 3, 5 and 7 for training and data-sets 2, 4 and 6 for testing. All test data was standardized before model fitting.

All models fit have approximately 118,000 parameters. That is, the RNN has 340 neurons, the LSTM has 170 neurons and the RENNs have width $n = 75$ and $q = 150$.

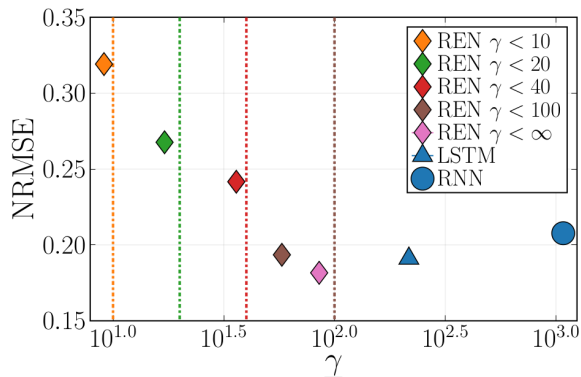


Fig. 2. Nominal performance versus robustness for models trained on F16 ground vibration benchmark dataset.

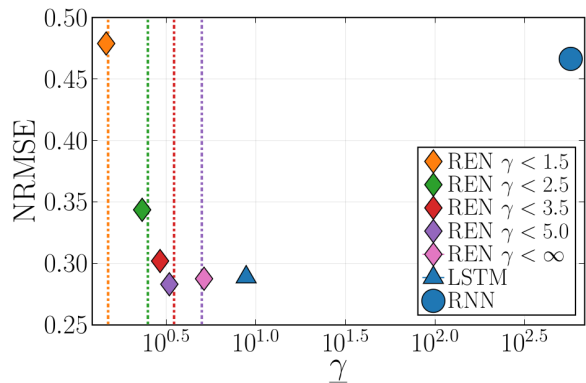


Fig. 3. Nominal performance versus robustness for models trained on Wiener-Hammerstein with process noise benchmark dataset.

Models were trained for 70 epochs with a sequence length of 1024. The learning rate was initialized at 1×10^3 and was reduced by a factor of 10 every 20 Epochs.

2) *Wiener-Hammerstein With Process Noise Benchmark:* The Wiener Hammerstein with process noise benchmark data-set [53] involves the estimation of the output voltage from two input voltage measurements for a block oriented Wiener-Hammerstein system with large process noise that complicates model fitting. We have used the Multi-sine fade-out data-set consisting of two realisations of a multi-sine input signal with 8192 samples each. The test set consists of two experiments, a random phase multi-sine and a sine sweep, conducted without the added process noise.

All models fit have approximately 42,000 parameters. That is, the RNN has 200 neurons, the lstm has 100 neurons and the RENs have $n = 40$ and $q = 100$. Models were trained for 60 epochs with a sequence length of 512. The initial learning rate was 1×10^{-3} . After 40 epochs, the learning rate was reduce to 1×10^{-4} .

B. Results and Discussion

We have plotted the mean test performance versus the observed sensitivity of the models trained on the F16 and Wiener-Hammerstein Benchmarks in figures 2 and 3 respectively. The dashed vertical lines show the guaranteed upper bounds on the Lipschitz constant for the bounded RENs. In all cases, we observe that REN provides the best trade-off between nominal performance and robustness with the REN slightly outperforming the LSTM in terms of nominal test error for large γ . By tuning γ , nominal test performance can be traded-off for robustness, signified by the consistent trend moving diagonally up and left with decreasing γ . In all cases, we found that the REN was significantly more robust than the RNN, typically having about 10% of the sensitivity for the F16 benchmark and 1% on the Wiener-Hammerstein benchmark. Also note that for small γ , the observed lower bound on the Lipschitz constant is very close to the guaranteed upper bound, showing that the real Lipschitz constant of the models is close to the upper bound.

We have also plotted an example output from the Wiener-Hammerstein Multi-sine Test data set in Fig. 4 for a subset

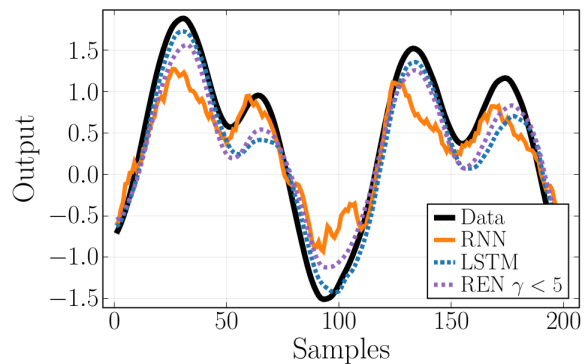


Fig. 4. Example trajectories from Wiener Hammerstein random phase multi-sine test dataset.

for the best performing REN, the LSTM and the RNN. The RNN displays sharp and erratic behaviour. The REN is guaranteed not to display this behaviour as the robustness constraints ensure smoothness of the trajectories.

Finally, we have plotted the loss versus the number of epochs in Fig. 5 for some of the models on the F16 dataset. Compared the LSTM, the REN takes a similar number of steps and achieves a slightly lower training loss. The LSTM is a model designed to be easy to train.

VI. CONCLUSIONS AND FUTURE WORK

In this paper we have introduced RENs as a new model class for learning dynamical systems with stability and robustness constraints. The model set is flexible and admit a direct parameterization, allowing learning via unconstrained optimization.

Testing on system identification benchmarks against the standard RNN and LSTM models showed that RENs can comparable or even slightly improved generalisation performance, and results in models with far lower sensitivity to input perturbations.

Our future work will explore uses of RENs beyond system identification. In particular, the results of [30] and [54] encourage the use of robust dynamical models for reinforcement learning of feedback controllers, whereas building on

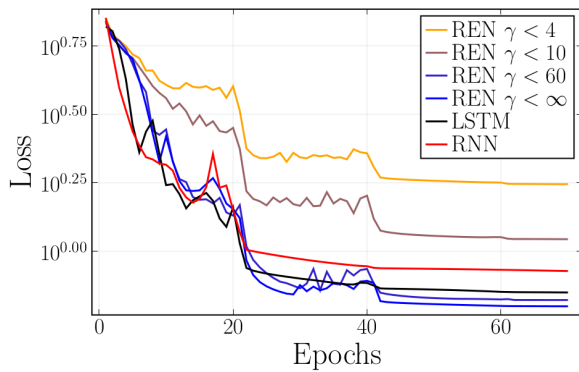


Fig. 5. Nominal performance versus robustness for models trained on F16 ground vibration benchmark dataset.

[55] with RENs one can optimize or learn robust observers (state estimators) for nonlinear dynamical systems.

REFERENCES

- [1] M. Schetzen, *The Volterra and Wiener Theories of Nonlinear Systems*. USA: Krieger Publishing Co., Inc., 2006.
- [2] T. B. Schön, A. Wills, and B. Ninness, "System identification of nonlinear state-space models," *Automatica*, vol. 47, no. 1, pp. 39–49, 2011.
- [3] S. A. Billings, *Nonlinear system identification: NARMAX methods in the time, frequency, and spatio-temporal domains*. John Wiley & Sons, 2013.
- [4] D. Mandic and J. Chambers, *Recurrent neural networks for prediction: learning algorithms, architectures and stability*. Wiley, 2001.
- [5] J. M. Maciejowski, "Guaranteed stability with subspace methods," *Systems & Control Letters*, vol. 26, no. 2, pp. 153–156, Sep. 1995.
- [6] T. Van Gestel, J. A. Suykens, P. Van Dooren, and B. De Moor, "Identification of stable models in subspace identification by using regularization," *IEEE Transactions on Automatic Control*, vol. 46, no. 9, pp. 1416–1420, 2001.
- [7] S. L. Lacy and D. S. Bernstein, "Subspace identification with guaranteed stability using constrained optimization," *IEEE Transactions on automatic control*, vol. 48, no. 7, pp. 1259–1263, 2003.
- [8] U. Nallasivam, B. Srinivasan, V. Kuppuraj, M. N. Karim, and R. Rengaswamy, "Computationally Efficient Identification of Global ARX Parameters With Guaranteed Stability," *IEEE Transactions on Automatic Control*, vol. 56, no. 6, pp. 1406–1411, Jun. 2011.
- [9] D. N. Miller and R. A. De Callafon, "Subspace identification with eigenvalue constraints," *Automatica*, vol. 49, no. 8, pp. 2468–2473, 2013.
- [10] J. Umenberger and I. R. Manchester, "Convex Bounds for Equation Error in Stable Nonlinear Identification," *IEEE Control Systems Letters*, vol. 3, no. 1, pp. 73–78, Jan. 2019.
- [11] G. Y. Mamakoukas, O. Xherija, and T. Murphey, "Memory-Efficient Learning of Stable Linear Dynamical Systems for Prediction and Control," *Advances in Neural Information Processing Systems*, vol. 33, pp. 13 527–13 538, 2020.
- [12] M. M. Tobenkin, I. R. Manchester, J. Wang, A. Megretski, and R. Tedrake, "Convex optimization in identification of stable non-linear state space models," in *49th IEEE Conference on Decision and Control (CDC)*. IEEE, 2010.
- [13] M. M. Tobenkin, I. R. Manchester, and A. Megretski, "Convex Parameterizations and Fidelity Bounds for Nonlinear Identification and Reduced-Order Modelling," *IEEE Transactions on Automatic Control*, vol. 62, no. 7, pp. 3679–3686, Jul. 2017.
- [14] J. Umenberger, J. Wagberg, I. R. Manchester, and T. B. Schön, "Maximum likelihood identification of stable linear dynamical systems," *Automatica*, vol. 96, pp. 280–292, 2018.
- [15] J. Umenberger and I. R. Manchester, "Specialized Interior-Point Algorithm for Stable Nonlinear System Identification," *IEEE Transactions on Automatic Control*, vol. 64, no. 6, pp. 2442–2456, 2018.
- [16] S. M. Khansari-Zadeh and A. Billard, "Learning Stable Nonlinear Dynamical Systems With Gaussian Mixture Models," *IEEE Transactions on Robotics*, vol. 27, no. 5, pp. 943–957, Oct. 2011.
- [17] J. Miller and M. Hardt, "Stable recurrent models," in *International Conference on Learning Representations*, 2019.
- [18] J. Z. Kolter and G. Manek, "Learning Stable Deep Dynamics Models," p. 9.
- [19] M. Revay and I. Manchester, "Contracting implicit recurrent neural networks: Stable models with improved trainability," in *Learning for Dynamics and Control*. PMLR, 2020, pp. 393–403.
- [20] M. Revay, R. Wang, and I. R. Manchester, "A convex parameterization of robust recurrent neural networks," *IEEE Control Systems Letters*, vol. 5, no. 4, pp. 1363–1368, 2021.
- [21] W. Lohmiller and J.-J. E. Slotine, "On contraction analysis for nonlinear systems," *Automatica*, vol. 34, pp. 683–696, 1998.
- [22] M. Cheng, J. Yi, P.-Y. Chen, H. Zhang, and C.-J. Hsieh, "Seq2sick: Evaluating the robustness of sequence-to-sequence models with adversarial examples," in *Association for the Advancement of Artificial Intelligence*, 2020, pp. 3601–3608.
- [23] C. A. Desoer and M. Vidyasagar, *Feedback systems: input-output properties*. SIAM, 1975, vol. 55.
- [24] P. L. Bartlett, D. J. Foster, and M. J. Telgarsky, "Spectrally-normalized margin bounds for neural networks," in *Advances in Neural Information Processing Systems*, 2017, pp. 6240–6249.
- [25] S. Zhou and A. P. Schoellig, "An analysis of the expressiveness of deep neural network architectures based on their lipschitz constants," *arXiv preprint arXiv:1912.11511*, 2019.
- [26] T. Huster, C.-Y. J. Chiang, and R. Chadha, "Limitations of the lipschitz constant as a defense against adversarial examples," in *Joint European Conference on Machine Learning and Knowledge Discovery in Databases*. Springer, 2018, pp. 16–29.
- [27] H. Qian and M. N. Wegman, "L2-nonexpansive neural networks," *International Conference on Learning Representations (ICLR)*, 2019.
- [28] H. Gouk, E. Frank, B. Pfahringer, and M. J. Cree, "Regularisation of neural networks by enforcing lipschitz continuity," *Machine Learning*, vol. 110, no. 2, pp. 393–416, 2021.
- [29] M. Revay and I. R. Manchester, "Contracting implicit recurrent neural networks: Stable models with improved trainability," *Learning for Dynamics and Control (LADC)*, 2020.
- [30] A. Russo and A. Proutiere, "Optimal attacks on reinforcement learning policies," *arXiv preprint arXiv:1907.13548*, 2019.
- [31] A. Virmaux and K. Scaman, "Lipschitz regularity of deep neural networks: analysis and efficient estimation," in *Advances in Neural Information Processing Systems*, S. Bengio, H. Wallach, H. Larochelle, K. Grauman, N. Cesa-Bianchi, and R. Garnett, Eds., vol. 31. Curran Associates, Inc., 2018.
- [32] M. Fazlyab, A. Robey, H. Hassani, M. Morari, and G. Pappas, "Efficient and accurate estimation of lipschitz constants for deep neural networks," in *Advances in Neural Information Processing Systems*, 2019, pp. 11 423–11 434.
- [33] P. Pauli, A. Koch, J. Berberich, P. Kohler, and F. Allgower, "Training robust neural networks using lipschitz bounds," *IEEE Control Systems Letters*, 2021.
- [34] S. Bai, J. Z. Kolter, and V. Koltun, "Deep equilibrium models," in *Advances in Neural Information Processing Systems*, 2019, pp. 690–701.
- [35] L. El Ghaoui, F. Gu, B. Travacca, A. Askari, and A. Y. Tsai, "Implicit deep learning," *arXiv:1908.06315*, 2019.
- [36] E. Winston and J. Z. Kolter, "Monotone operator equilibrium networks," *arXiv:2006.08591*, 2020.
- [37] M. Revay, R. Wang, and I. R. Manchester, "Lipschitz bounded equilibrium networks," *arXiv:2010.01732*, 2020.
- [38] S. Hochreiter and J. Schmidhuber, "Long Short-Term Memory," *Neural computation*, vol. 9, pp. 1735–1780, 1997.
- [39] M. M. Tobenkin, I. R. Manchester, and A. Megretski, "Convex parameterizations and fidelity bounds for nonlinear identification and reduced-order modelling," *IEEE Transactions on Automatic Control*, vol. 62, no. 7, pp. 3679–3686, 2017.
- [40] I. Goodfellow, Y. Bengio, and A. Courville, *Deep learning*. MIT press, 2016.
- [41] E. K. Ryu and S. Boyd, "Primer on monotone operator methods," *Appl. Comput. Math*, vol. 15, no. 1, pp. 3–43, 2016.
- [42] A. Megretski and A. Rantzer, "System analysis via integral quadratic constraints," *IEEE Trans. Autom. Control*, vol. 42, no. 6, pp. 819–830, Jun. 1997.

- [43] Y.-C. Chu and K. Glover, "Bounds of the induced norm and model reduction errors for systems with repeated scalar nonlinearities," *IEEE Transactions on Automatic Control*, vol. 44, no. 3, pp. 471–483, 1999.
- [44] F. J. D'Amato, M. A. Rotea, A. Megretski, and U. Jönsson, "New results for analysis of systems with repeated nonlinearities," *Automatica*, vol. 37, no. 5, pp. 739–747, 2001.
- [45] V. V. Kulkarni and M. G. Safonov, "All multipliers for repeated monotone nonlinearities," *IEEE Transactions on Automatic Control*, vol. 47, no. 7, pp. 1209–1212, 2002.
- [46] M. Schoukens and K. Tiels, "Identification of block-oriented nonlinear systems starting from linear approximations: A survey," *Automatica*, vol. 85, pp. 272–292, 2017.
- [47] F. Giri and E.-W. Bai, *Block-oriented nonlinear system identification*. Springer, 2010, vol. 1.
- [48] M. Schoukens, A. Marconato, R. Pintelon, G. Vandersteen, and Y. Rolain, "Parametric identification of parallel wiener-hammerstein systems," *Automatica*, vol. 51, pp. 111–122, 2015.
- [49] J. Noël and M. Schoukens, "F-16 aircraft benchmark based on ground vibration test data," *Workshop on Nonlinear System Identification Benchmarks*, pp. 15–19, 2017.
- [50] M. Schoukens and J. Noël, "Wiener-hammerstein benchmark with process noise," *Workshop on Nonlinear System Identification Benchmarks*, pp. 19–23, 2017.
- [51] D. P. Kingma and J. Ba, "Adam: A Method for Stochastic Optimization," *International Conference for Learning Representations (ICLR)*, Jan. 2017.
- [52] M. Innes, "Don't unroll adjoint: Differentiating ssa-form programs," *arXiv preprint arXiv:1810.07951*, 2018.
- [53] M. Schoukens and J. Noël, "Wiener-hammerstein benchmark with process noise," in *Workshop on nonlinear system identification benchmarks*, 2016, pp. 15–19.
- [54] R. Wang and I. R. Manchester, "Robust contraction analysis of nonlinear systems via differential iqc," in *2019 IEEE 58th Conference on Decision and Control (CDC)*. IEEE, 2019, pp. 6766–6771.
- [55] I. R. Manchester, "Contracting nonlinear observers: Convex optimization and learning from data," in *2018 Annual American Control Conference (ACC)*. IEEE, 2018, pp. 1873–1880.